Room Temperature Electroreductive Carboxylation of Unactivated Alkyl Chlorides with CO_2 Using a Ni(II) NNN-Pincer Complex. Towards Polyvinyl chloride (PVC) Upgrading

Prasenjit Sarkar[†,§], Sandeep Dash[#,§], Jeanette A. Krause[†], Julien A. Panetier[#]*, Jianbing "Jimmy" Jiang[†]*

[†]Department of Chemistry, University of Cincinnati, P.O. Box 210172, Cincinnati, Ohio 45221, United States

Department of Chemistry, State University of New York at Binghamton, Binghamton, NY 13902 United States

[§] The authors contributed equally.

*Corresponding author: Email: jianbing.jiang@uc.edu

*Corresponding author: Email: panetier@binghamton.edu

TOC Graphic

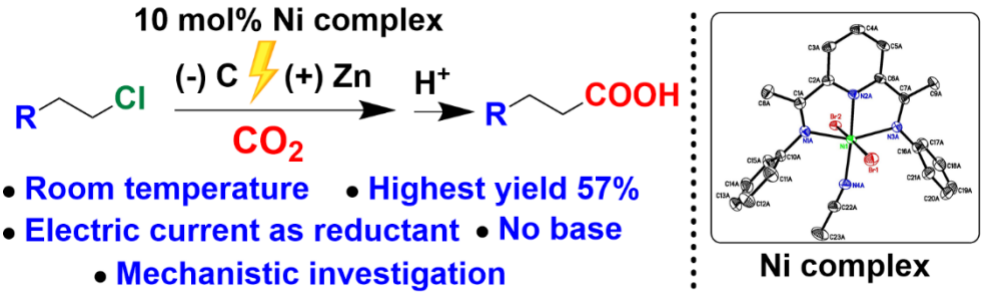

An experimental and computational investigation on the electrochemical carboxylation of a wide range of unactivated alkyl chlorides by a nickel pincer complex

Abstract

In organic synthesis, direct carboxylation of organohalides with carbon dioxide is a highly desirable transformation because it uses feedstock chemicals and produces carboxylic acids, which are among the most widely used classes of organic compounds. Alkyl carboxylic acids are favored motifs in many medicines and physiologically active substances. Carbon dioxide (CO_2) is an ideal C1 source for organic synthesis because of its high abundance, low cost, nontoxicity, and recyclability. This article describes a nickel-catalyzed electrochemical method for producing alkyl carboxylic acids via carboxylation of unactivated alkyl chlorides with CO_2. The development of a Ni pincer complex (complex **1**) with a redox-active ligand as an electrocatalyst to convert unactivated alkyl chlorides to the corresponding acids over less desirable homocoupling products is presented. Electronic structure calculations revealed that CO_2 binding occurs in a resting state to yield an η^2-CO_2 adduct and that the C–Cl bond activation step is the TOF-determining transition state, which has an activation energy of 19.3 kcal/mol. A combination of electroanalytical methods, control experiments, and computational studies revealed the mechanism of the electrocarboxylation reaction. In addition, complex **1** has been demonstrated as an efficient catalyst to upgrade polyvinyl chloride to polyacrylate in 95% yield.

1. Introduction

Reductive C–C bond-forming reactions are effective in building molecular systems. Cross-coupling reactions are valuable tools for generating C–C bonds by avoiding additional synthetic steps and using moisture-sensitive organometallic reagents.[1] For several decades, transition metal catalysis[2-6] and photocatalysis[7-13] have been developed to expand the coupling ability of such reactions. The development of electrochemistry[14-21] in recent years has allowed the utilization of electrons in reductive cross-coupling reactions. Electrocatalysis is a crucial tool in this endeavor because of its low potential, less hazardous reaction conditions, and a wide range of functional group tolerances. Group 10 metals (Ni, Pd, and Pt) are mainly used for catalyst selection. However, less costly Ni-based electrocatalysts are gaining attention for electroreductive couplings.[22-26] Since last decades several research groups have investigated carboxylation of phenyl, benzylic, allyl, and alkyl substrates both chemically and electrochemically.[24,27-32] In 2013 and 2016, Martin group reported chemically carboxylation of benzylic halides and also unactivated alkyl chlorides using a Ni catalyst.[27,29] They demonstrated the carboxylation of unactivated alkyl chorides at 60 °C temperature (**Figure 1**). The Lu group in 2014 reported Co^{II}-salen catalyst for the electrochemical carboxylation of benzylic chlorides (**Figure 1**).[28] Recently, Ackermann group reported an electrochemical pathway to carboxylate activated phenyl allylic chloride using Co catalyst (**Figure 1**).[30] Interestingly, Manthiram and co-workers presented an electrocarboxylation of alkyl chlorides by using 20 mA of CCE but with low product yields (**Figure 1**).[33] More recently, Yu *et al.* reported an electroreductive Ni catalyst system for the carboxylation of unactivated aryl chlorides and unactivated alkyl bromides (**Figure 1**).[34] The perception that unactivated alkyl chlorides cannot be used in cross-electrophile events persists even though notably complex transformations have been developed. These include the formidably high activation energy required to significantly affect $C(sp^3)$–Cl cleavage and the inherent proclivity of alkyl metal species toward β-hydride elimination or homocoupling pathways. However, if successful, this unexplored territory would open the door to organic synthesis with polyhalogenated backbones, significantly enhancing our ever-expanding synthetic portfolio.

Carboxylic acids are a predominant functional group in biologically related compounds, natural products, and pharmaceuticals.[35-37] They are typically synthesized by the oxidation of alcohols or aldehydes and the hydrolysis of nitriles. However, in recent years, electroreductive coupling reactions with carbon dioxide (CO_2) have received particular attention for the synthesis of high-value carboxylic acids from straightforward and easily accessible precursors.[38-44] Owing

to their appealing chemical properties, such as abundance, affordability, nontoxicity, and renewable nature, carbon dioxide (CO_2), a fundamental C1 building component, has gained considerable synthetic interest. Developing an innovative and reliable CO_2-fixation process to produce high value-added carboxylic acids from straightforward starting materials is highly desirable given the growing importance of carbon neutrality.

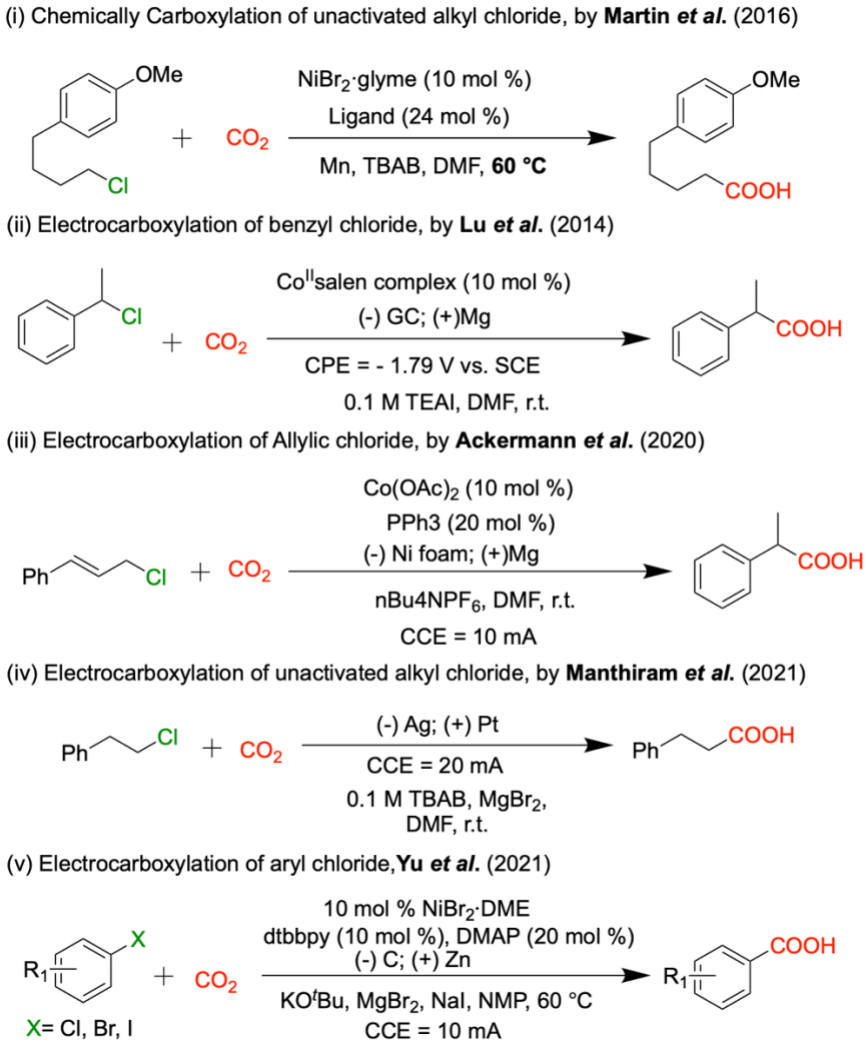

Figure 1. Carboxylation of different C–Cl substrates.

As part of our ongoing interest in electrochemistry using transition metal catalysts, we developed a simple and convenient process using an undivided electrochemical cell with a carbon felt cathode and Zn anode. This simplistic cell was used to avoid the high cost and impracticality of membrane separation. Recent studies on electrocarboxylation[34,45] using a Ni complex with bidentate ligands encouraged us to expand our research to alkyl carboxylation. Herein, a redox-active ligand[46] containing a Ni-pincer complex precatalyst for the

electrochemical carboxylation of unactivated alkyl chlorides with CO_2 is reported for the first time (**Figure 1B**). Moreover, various primary unactivated alkyl substrates exhibited good carboxylic acid formation. A computational study using density functional theory (DFT) was performed to determine the mechanistic pathway of the reaction. Furthermore, the catalyst has been demonstrated to upcycle polyvinyl chloride (PVC) to polyacrylate in 95% yield.

2. Results and discussion

2.1 Synthesis

To understand their electrocarboxylative catalytic behavior, four nickel complexes were synthesized by reacting equivalent amounts of the ligand and $NiBr_2$ in excellent yields (See Supporting Information for details). Electrospray ionization-mass spectrometry (ESI-MS) and infrared spectroscopy were used to characterize these complexes. Single-crystal X-ray diffraction (SCXRD) was used to determine the molecular structure of the unsubstituted complex, **1**. Two types of crystals of **1** were obtained from the acetonitrile-diethyl ether solution: dark red and orange block-shaped crystals. Analysis of the dark-red crystals revealed a monoclinic $P2_1/c$ packing arrangement with two independent molecules in the asymmetric unit (**1-m**). The orange crystals adopted an orthorhombic *Pbca* arrangement with one independent molecule (**1-o**). Both forms crystallize as acetonitrile solvates. The molecular structure of Molecule A of **1-m** is presented in **Figure 2B** (Molecule B, the second independent molecule of **1-m** and the structure of **1-o** are shown in **Figure S1** and **Figure S2**). The crystallographic parameters and bonding metrics of **1-m** and **1-o** are listed in **Tables S1-S3.** The structural elucidation of complex **1** revealed an octahedral geometry around the Ni center with the chelating ligand, two bromine atoms situated *trans* to each other, and a terminally bound CH_3CN group. The phenyl rings of the imine moieties are positioned such that they approach a perpendicular rather than an in-plane configuration (**1-m**: 63.1(8)-68.0(7)° for both independent molecules; **1-o**: 56.4(8)-66.2(9)°).

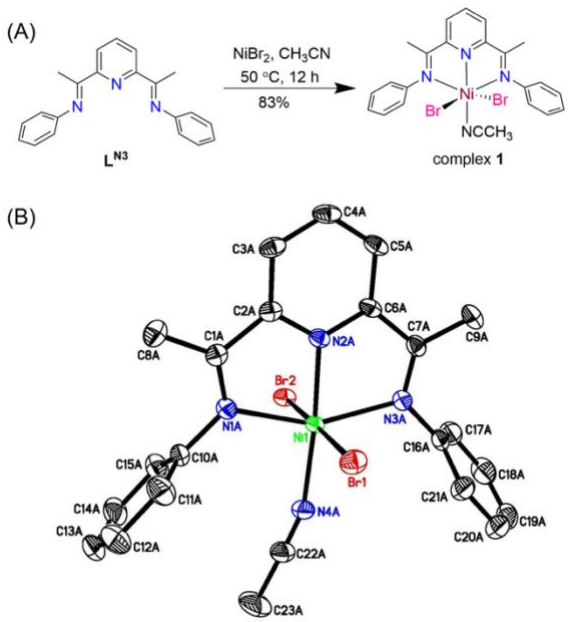

Figure 2. (A) Schematic representation for the synthesis of complex **1**. (B) Molecular structure of molecule A of **1-m**, drawn with 50% probability ellipsoids. Hydrogen atoms and lattice solvent are omitted for clarity.

2.2 Catalyst screening for electrochemical carboxylation

To understand the electrocatalytic behavior of the Ni complex, we employed 2-chloroethylbenzene as a model substrate. We examined nickel complexes of three tridentate ligands with a variety of electron-rich and electron-deficient substituents and one bidentate ligand. Interestingly, the electrocarboxylation of unactivated alkyl chlorides was previously observed in very low yields.[33] Thus, insights into carboxylation may not be straightforward. We hypothesized that (a) a tridentate ligand rather than a bidentate ligand might stabilize the substrate-bound complex, (b) the redox-active nature of the ligand might enhance electron transfer and contribute to the catalytic process, and (c) the introduction of substituents might favor carboxylation. After extensive optimization, we observed that the steric and electronic behavior of the ligand backbone possibly affected the formation of the intermediate (substrate-bound complex), which is critical for product formation and the suppression of side reactions (CO_2 reduction and homocoupling). Finally, we found that complex **1** showed the best electrocarboxylation performance (**Figure 3**).

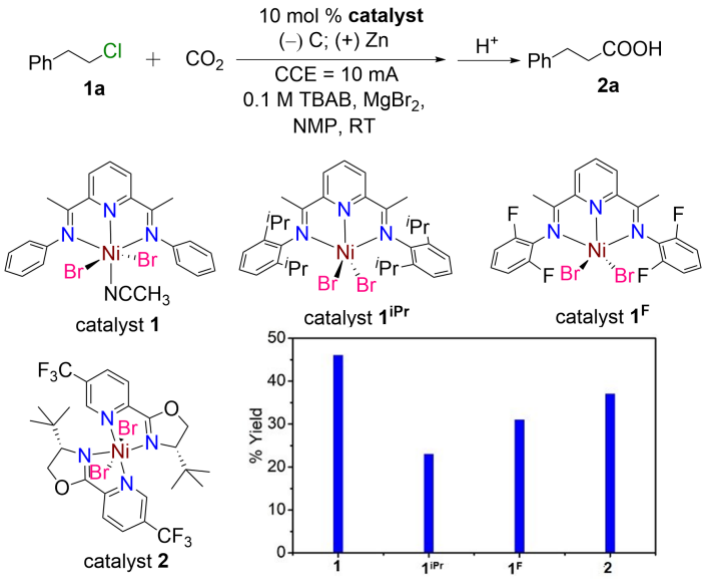

Figure 3. Development of a selective Ni-catalyzed electrochemical carboxylation reaction (undivided cell).

2.3 Reaction conditions, substrate scope, and limitations

To test the feasibility of this carboxylation strategy, phenylethyl chloride 1a was selected as the template alkyl chloride substrate to couple with CO_2 (**Table 1**). Using the combination of complex 1, $ZnBr_2$, 0.1 TBAB in NMP using carbon felt cathode and Zn anode at room temperature under 10 mA CCE, the desired carboxylic product 2a was obtained in 46% yield (**entry 1 in Table 1**). A series of control reactions were conducted to understand the role of each element. It was found that complex, current and $ZnBr_2$ Mn were all essential to this crosscoupling transformation (**entries 2−6**). Ni(II) salts such as $NiBr_2$ and $Ni(acac)_2$ were not efficient to promote the desired reaction as shown in **entry 3**. The homocoupling product was observed when a higher current (15 mA) was introduced (**entry 8**) in a decreased product yield. Gas chromatography−mass spectrometry (GCMS) analysis of the reaction mixture indicated that acid product significantly decreased due to the formation of homocoupling product. It was hypothesized that at a higher current, the phenyl ethyl radical was generated at a sufficient local concentration to favor dimerization. Switching to other solvents such as DMF (**entry 9**) and other electrolytes such as $TBAPF_6$ (**entry 10**) led to drastically reduced product formation.

Table 1. Optimization of electrocarboxylation reaction.

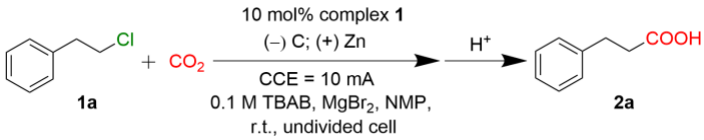

Entry	Conditions Varied	Yields of 2a (%)
1	None	46
2	w/o complex **1**	0
3	Using $Ni(acac)_2/NiBr_2$	5
4	w/o $MgBr_2$	13
5	w/o CO_2	0
6	w/o current	0
7	8 mA	24
8	15 mA	15
9	DMF as solvent	17
10	$TBAPF_6$ instead of TBAB	10

We then investigated the scope of the electrocarboxylation reaction using various alkyl chlorides (**Figure 4**). Phenyl alkyl chlorides with two or three alkyl chains afforded the desired carboxylic acids in good-to-moderate yield. Acyclic alkyl chlorides also provided important carboxylic acids in moderate yields. To diversify the substrate variations, heterocycle-containing alkyl chlorides such as thiophene (**1g**), ester (**1k**), and methoxy (**1d**) were considered and were found to be tolerated, producing the corresponding carboxylic acids in moderate yields. These results further supported the general utility of our method in medicinal chemistry. However, the limitations of this optimized method were observed when secondary or tertiary alkyl chlorides were used. Secondary alkyl chloride (**1i**) gave the desired product in 14% yield, whereas tertiary alkyl chloride (**1f**) resulted in only a trace amount. In these cases, the unreacted substrates remained the major components, with trace amounts of homocoupling products, as identified by GC-MS analysis of the crude reaction mixture. Previous studies have reported that aryl chlorides also produce low yields.[28] The steric requirements of the ligand phenyl substituents on the catalyst presumably play a role in the less favorable substrate.

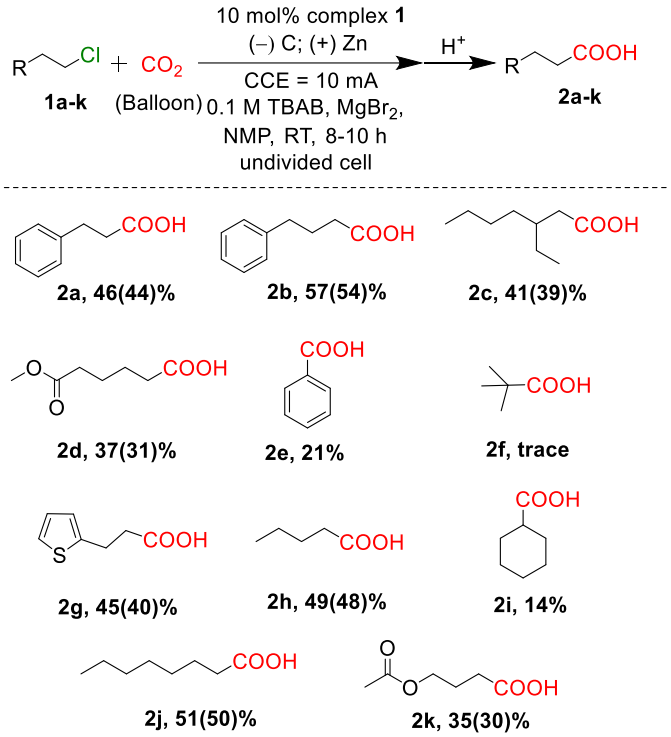

Figure 4. Reaction conditions and substrate scope; product yields are determined by ^{1}H NMR spectroscopy using ethylene carbonate as internal standard and isolated yields are given in brackets.

2.4 Mechanistic Studies

In preliminary mechanistic studies, 2-chloroethyl benzene was chosen as a model substrate to investigate the formation of carboxylation products because of its uncomplicated ^{1}H NMR pattern and small structural units. The homocoupling product was observed when a higher current (15 mA) was introduced, and it was speculated that at a higher current, the phenyl ethyl radical was generated at a sufficient local concentration to favor dimerization. We conducted control experiments with other solvents (DMF, MeCN) and electrolytes ($TBAPF_6$, NaI) but failed to achieve better results for reasons such as a small potential window and passivation. $MgBr_2$ was essential for obtaining the desired carboxylic acid product. Without the Mg salt, small amounts of organic carbonate and alcohol were formed, possibly because of the nucleophilic attack of the carbonate on the substrate. In the absence of a sacrificial anode, product formation was drastically reduced to trace amounts. A disadvantage observed when sacrificial anodes for carboxylation were used: the precipitation of inorganic carbonates, which can decrease the cell potential. During electrolysis, $MgCO_3$ and $ZnCO_3$ are generated, as observed by attenuated

total reflectance (ATR) spectroscopy (**Figure S7**), which can passivate the cathode. When used, 1-methyl-2-pyrrolidinone (NMP) dissolves a significant amount of inorganic carbonates, which helps prevent premature reaction stoppage by exceeding the voltage limit. During the reaction process, Cl^- was eliminated from the medium as confirmed by ion chromatography (IC) measurements (**Figure S8**).

Control experiments were performed to elucidate the reaction process (**Figure S9**). We introduced $Ni(COD)_2$ and ligand $\mathbf{[L^{N3}]^H}$ as catalysts, which resulted in 18% product yield, a lower yield than that with precatalyst **1**. Additionally, we performed a current electrolysis control experiment with **1a** in the absence of CO_2 and found only a homocoupling product. Prompted by this observation, we introduced 2,2,6,6-tetramethylpiperidin-1-yl)oxyl (TEMPO) into the reaction and observed no carboxylic acid products. However, a TEMPO-bound **1a** radical was detected by high-resolution mass spectrometry (HRMS) (**Figure S10**). Thus, radical formation is an essential step in the reaction.

Various electrochemical analyses were conducted to gain further insights into the reaction mechanism. The cyclic voltammogram (CV) of complex **1** (**Figure 5**) shows several reduction redox waves, including ligand-centered (imine reduction) and metal-centered reductions. The first reduction peak at –1.22 V vs. Fc/Fc^+ was attributed to the ligand reduction, while the second peak at –1.59 V vs. Fc/Fc^+ was possibly due to the reduction of Ni(II) to Ni(I) and has been confirmed by electronic structure calculations (*vide infra*).

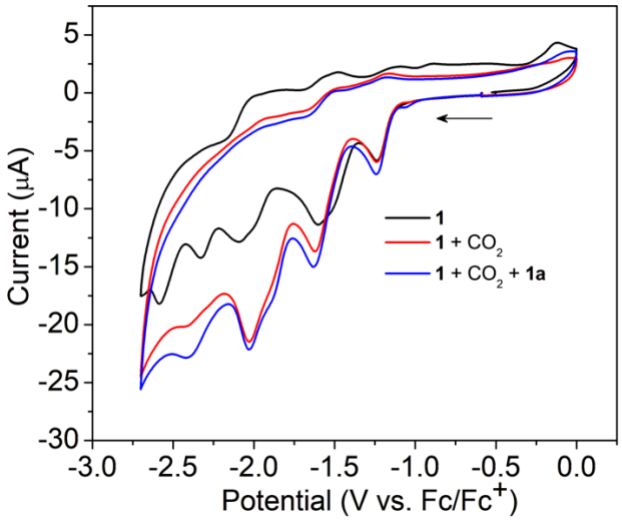

Figure 5. Cyclic voltammetry traces of the system with complex **1** (black), the system with CO_2 addition to complex **1** (red), and the system after the addition of **1a** after the addition of CO_2 (blue).

Mechanistically, one can envision two active routes leading to a C-C cross-coupled product. The precatalyst either (1) electrochemically generates an active Ni(I) species with two successive one-electron reductions, which can react with the alkyl chloride by oxidative addition, followed by CO_2 insertion and reductive elimination, or (2) the complex initially undergoes a two-electron reduction to generate a Ni(I) radical species that reacts with CO_2 and, upon elimination, results in the final acid product. The experimental detection (**Figure S10**) of a TEMPO-bound alkyl unit during electrolysis in the presence of TEMPO supports the notion that a radical is formed as an intermediate. A chemical reduction experiment was conducted by reacting KC_8 (2 equiv.) with complex **1** to generate a two-electron-reduced Ni complex. Subsequently, the reduced species reacted separately with CO_2 and **1a**. Both solutions were subjected to HR-ESIMS to form either the (2-R) **1**-**1a** adduct or the **2**-CO_2 adduct; however, the desired species were not observed. If a CO_2-adduct was formed, it would be difficult to detect, as the process may be reversible and binding weak, which was also computationally investigated (*vide infra*). Interestingly, we observed a distinct color change from brown to green upon purging the reduced species with CO_2 whereas purging **1a** with CO_2 resulted in no color change. This suggests that the two-electron reduced Ni complex reacts promptly with CO_2. Moreover, the addition of 20 equiv of **1a** showed no change in the current for either the 1st or 2nd reduction peaks in the CV. Addition of the substrate did not shift the second peak. However, there was an increase in the current at higher negative potentials {i.e., at –2.56 V (**Figure S11A**)}. Purging with CO_2 prior to substrate addition increased and shifted the second reduction peak to –1.62 V. This observation supported the formation of a CO_2-bound complex. However, there was little change in the electrochemical behavior after substrate introduction because of low substrate reactivity. It was postulated that the incorporation of CO_2 results in the formation of carboxylate intermediates.

2.5 Computational Results

2.5.1. Formation of the Resting State

Density functional theory (DFT) calculations were performed to further investigate the electroreductive carboxylation of **1a** in the presence of complex **1**. This catalyst was chosen due to its efficient electrocarboxylation performance (**Figure 3**). Our results indicate that **1** has a triplet ground state (S = 1, **Table S4**), where the Mulliken spin on Ni approaches that of 2 (ρ_{Ni} = 1.6, **Figure 6**), which is consistent with the Ni(II) metal center (d^8 electronic configuration).

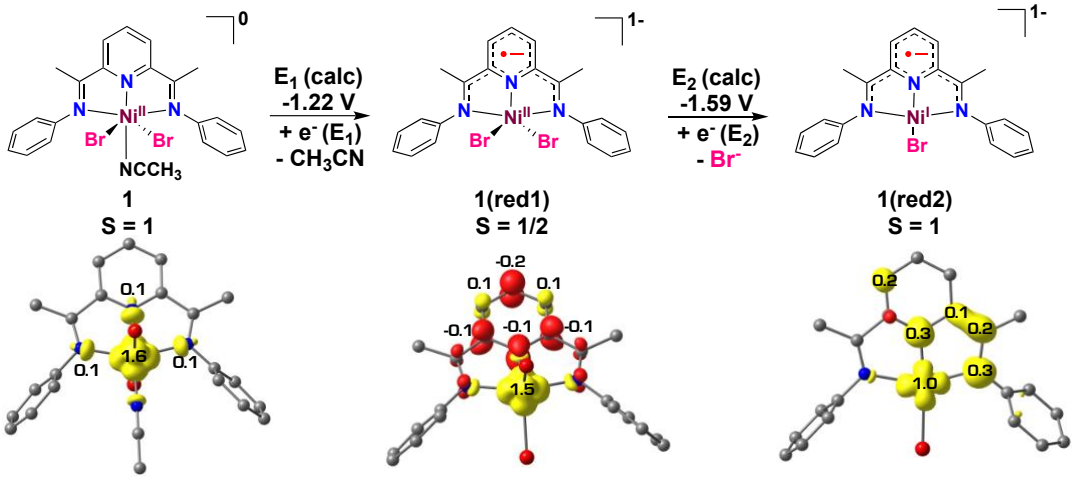

Figure 6. Computed redox potentials (in V vs. Fc/Fc^+) for the one- and two-electron reduced species and isosurface (0.007 a.u.) plots of the Mulliken spin.

Following the optimization of **1**, we considered various possibilities for the one- and two-electron-reduced species (**Tables S5-6** and **Figure S13-14**). For instance, bromine and acetonitrile could dissociate after the first reduction step through a stepwise or concerted process (**Tables S5** and **Figure S13**). Our DFT calculations implied that acetonitrile dissociation to yield the trigonal bipyramidal complex **1(red1)** through a concerted process was slightly more favorable (**Figure 6**). The redox potential for this initial reaction of –1.22 V versus the Fc/Fc^+ couple agrees with the cyclic voltammetry traces of complex **1** (**Figure 5**). Interestingly, the first reduction is ligand-centered, where the Mulliken spin on Ni remains unchanged (i.e., ρ_{Ni} = 1.5 in **1(red1)** *cf.* ρ_{Ni} = 1.6 in complex **1**). In this electronic configuration, both the unpaired electrons on Ni are antiferromagnetically coupled with one electron on the ligand to yield a doublet ground state (**Table S5**).

In the case of the second reduction event, our calculations reveal that the metal center is reduced at –1.59 V, signifying that the resting state, **1(red2)**, is best described as a nickel(I) metal center that is ferromagnetically coupled with an unpaired electron on the ligand (**Figure 6**).

2.5.2. CO_2 binding versus C-Cl bond activation at 1(red2).

Following the generation of **1(red2)**, multiple pathways for CO_2 binding and C–Cl bond activation of **1a**, with or without the prior dissociation of bromine, were explored (**Figure S15**). If the lowest energy pathways, without initial bromine dissociation at the four-coordinated species **1(red2)** are considered (**Figure 7A**), our calculations show that the C–Cl bond activation

requires an activation energy of 19.2 kcal/mol relative to the separated reactants. Interestingly, the computed transition indicates nucleophilic attack of the metal center (Ni□C = 2.51 Å, **Figure 7C**) at the alkyl halide carbon atom (C□Cl = 2.26 Å). The first pathway is exergonic by 24.9 kcal/mol.

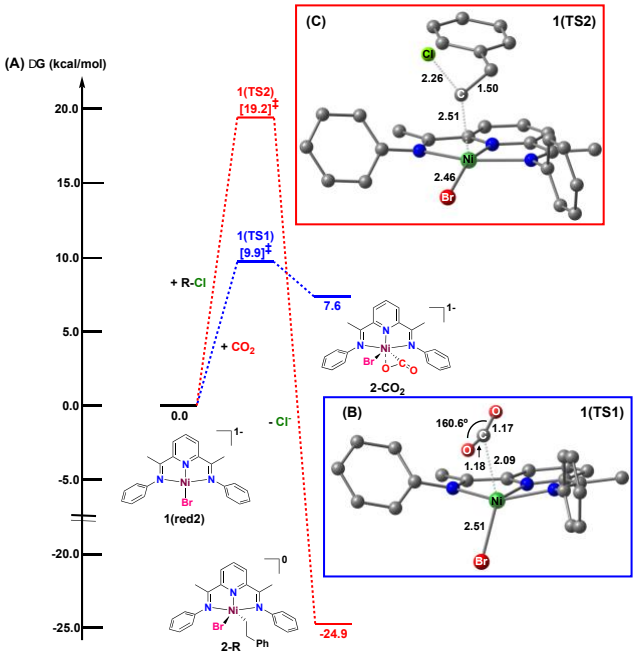

Figure 7. (A) Computed free energy (kcal/mol) profile for CO_2 binding and the C–Cl bond activation of **1a**. All free energies are calculated relative to the separated reactants. (B) Optimized transition state **1(TS1)** for CO_2 binding. (C) Optimized transition state **1(TS2)** for C–Cl bond activation of **1a**. Distances are in angstroms (Å), and the bond angle is in degrees (°). Non-participating hydrogen atoms are omitted for clarity. All complexes have a triplet ground state.

We also identified a second pathway in which CO_2 binds to **1(red2)** (**Figure 7A**). In this pathway, yielding an η^2-CO_2-adduct (**2-CO₂**) is kinetically more favorable than C–Cl bond cleavage by 9.3 kcal/mol. Forming a CO_2-bound complex after the second reduction event is preferred; however, this alternative pathway is endergonic by 7.6 kcal/mol, implying that the process may be reversible without further reduction events. This was consistent with the HR-ESI-MS and electrochemical data (**Figure 5**).

2.5.3. Cross-coupling carboxylation and product release.

Based on the CV results, we propose that additional reduction events after **2-CO₂** are required before the C-Cl bond activation of **1a** (**Figure 5**). Adding one electron to **2-CO₂**, –1.90

V versus Fc/Fc^{+}, yields a distorted square-based pyramidal compound, denoted **3-CO_2**, upon bromine dissociation (ΔG = 3.5 kcal/mol, **Figure 8A**). The square planar geometry of **4-CO_2** was also possible following the dissociation of one arm of the imine ligand (Ni□N = 4.10 Å, **Figure 8C**). Intermediate **4-CO_2** features a nickel(0) metal center (ρ_{Ni} = 0.0, **Table S8**), which is 5.7 kcal/mol lower in energy than **3-CO_2** and requires an activation energy of 6.0 kcal/mol {**1(TS3)**, **Figure 8B**}. This species displays parameters similar to those of the metallocarboxyltae adduct reported by Hillhouse and co-workers.[47]

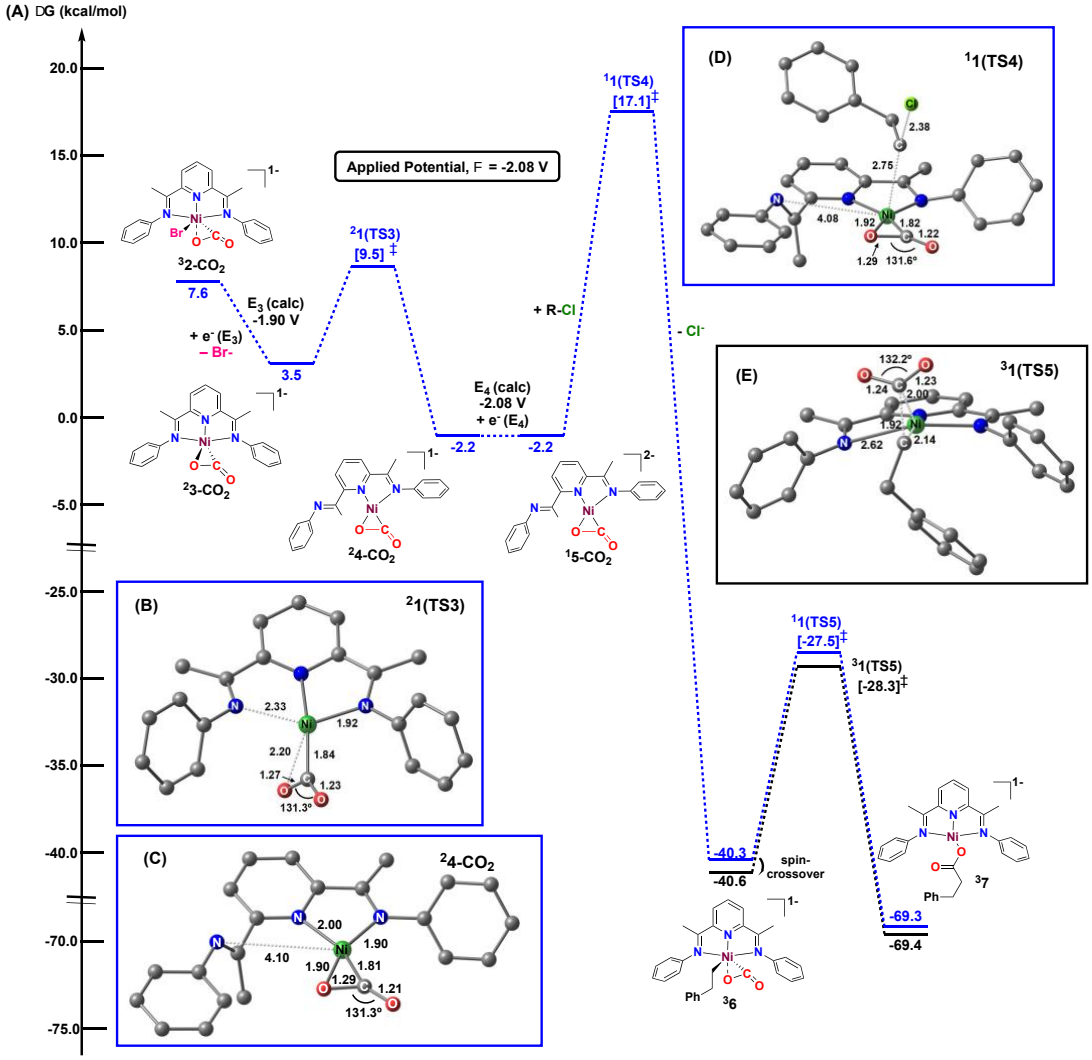

Figure 8. (A) Computed free energy (kcal/mol) profile for the cross-coupling carboxylation step. (B) Computed transition state **1(TS3)** for ligand dissociation. (C) Computed geometry for the Ni(0)-η^2-CO_2 adduct **4-CO_2**. (D) Transition state **1(TS4)** for the C–Cl bond activation at the Ni(0)-η^2-CO_2 adduct **5-CO_2**. (E) Computed transition state **1(TS5)** for the C–C cross-coupling step on the triplet surface. Distances are in angstroms, and the bond angles are in degrees. Non-

participating hydrogen atoms are omitted for clarity. The superscript represents the spin multiplicity of a given species.

After the formation of **4-CO$_2$**, two main pathways were hypothesized: (i) C–Cl bond cleavage can occur at **4-CO$_2$** followed by a fourth reduction before the C–C coupling event, or (ii) **4-CO$_2$** can be further reduced to give **5-CO$_2$** followed by activation of the alkyl chloride and the cross-coupling carboxylation step. Herein, we consider pathway (ii), which was found to be lower in energy (**Figure 8** and **Figure S16**).

Electronic structure calculations showed that the C–Cl bond cleavage of the alkyl chloride **1a** is more facile after a fourth reduction at –2.08 V to give **5-CO$_2$**. Again, the computed redox potential agrees with the experimental CV results (**Figure 5**). In this case, the activation energy was 19.3 kcal/mol relative to the infinitely separated reactants. Interestingly, the lowest energy transition state, which has a singlet ground state {ρ_{Ni} = 0.0 in **1(TS4)**}, shows that the imine ligand is partially dissociated (Ni□N = 2.51 Å, **Figure 8D**) and facilitates the activation of **1a** (Ni□C = 2.75 Å and C□Cl = 2.38 Å). We hypothesized that the stabilization of **1(TS4)** originates from the π-stacking interaction between the imine ligand and the phenyl group of the alkyl chloride, as shown by reduced density gradient (RDG) analysis (**Figure S17**). It should also be mentioned that the activation energy of 19.3 kcal/mol for **1(TS4)** is comparable to that of the C–Cl bond activation of **1a** at the resting state ($\Delta G^{\ddagger}$ = 19.2 kcal/mol, **1(TS2)**, **Figure 7A**). However, based on the HR-ESI-MS and electrochemical data (**Figure 5**), we believe that CO_2 binding occurs before the activation of the alkyl halide.

Following the cleavage of the C–Cl bond of **1a**, we located a transition state for the C–C bond cross-coupling step. Since the TOF-determining transition state **1(TS4)** is on a singlet surface and the resting state has a triplet ground state, we considered both singlet and triplet spin multiplicities (**Table S9**). As shown in **Figure 8A**, the activation energy on the triplet surface is slightly lower in energy, suggesting that the C–C cross-coupling step is preceded by spin-crossover to yield **6** in a triplet state (S = 1). In this case, the transition state **1(TS5)** reveals that one nitrogen atom of the imine ligand weakly interacted with the metal center (Ni□N = 2.62 Å, **Figure 8E**), while a C–C bond between CO_2 and the alkyl group is formed (C□C = 1.92 Å). With respect to **6** (S = 1), the process is exergonic by 28.8 kcal/mol. The final step of our proposed mechanism (not shown in **Figure 8A**) is the regeneration of the resting state in the presence of $MgBr_2$ (**Figure 9**), which is downhill by 19.8 kcal/mol, implying that the Gibbs free energy of reaction (ΔG_r) for the overall process is –89.2 kcal/mol.

Based on the experimental and computational data, we proposed a reaction mechanism for the electroreductive carboxylation of **1a** in the presence of **1** (**Figure 9**). Two redox events at −1.22 V and −1.59 V versus Fc/Fc^+ are needed to generate the resting state, **1(red2)**, from which CO_2 can bind to give the η^2-CO_2-adduct intermediate **2-CO_2**. This step occurs at an activation energy of 9.9 kcal/mol. After obtaining the metallocarboxylate intermediate, two additional redox events are necessary before the C−Cl bond cleavage of alkyl chloride **1a**. Our calculations indicate that this last step is the TOF-determining transition state (TDTS) with an activation energy of 19.3 kcal/mol. This transition state involves the radical character of the alkyl chloride, consistent with the experimental evidence that TEMPO can bind the alkyl unit during electrocatalysis. From **6**, the cross-coupling carboxylation step occurs, and the release of the final product is facilitated in the presence of $MgBr_2$ to regenerate resting-state **1(red2)**.

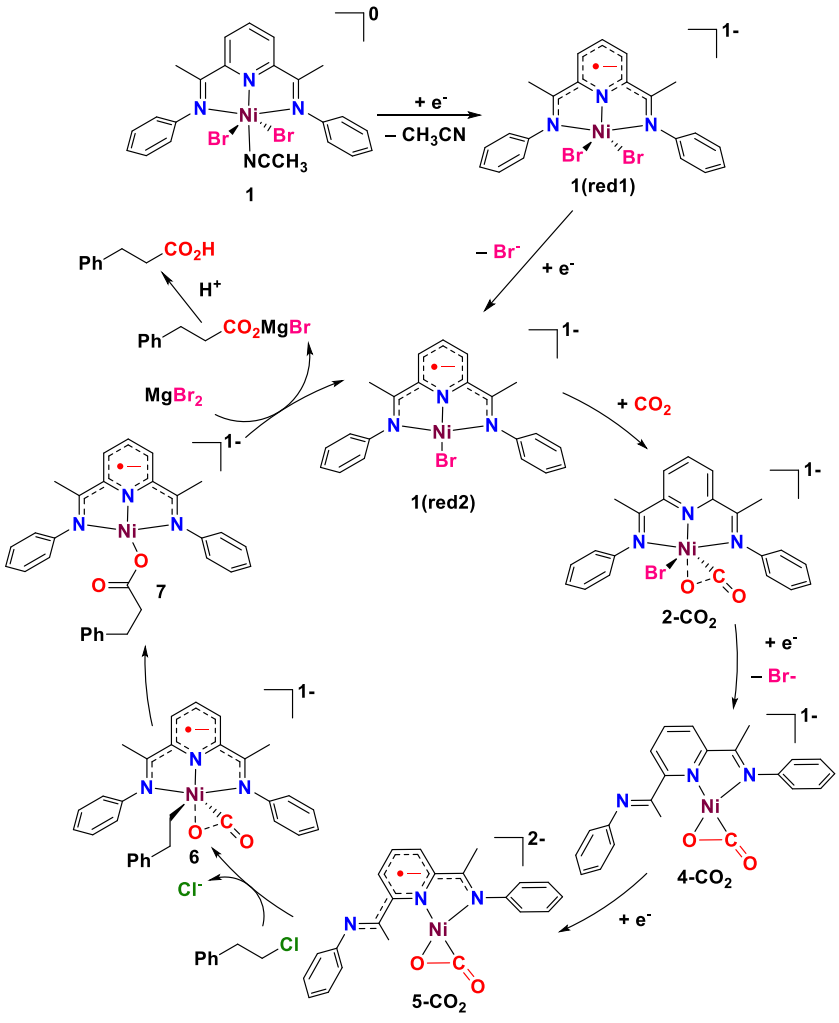

Figure 9. Plausible reaction mechanism for the electroreductive carboxylation of **1a** in the presence of complex **1**.

2.6. Electrocatalytic PVC upcycling activity of complex 1 via C–Cl activation

We continued the study to dechlorinate PVC followed by carboxylation using complex **1**. Initial the experiments with same conditions at room temperature yielded 5% of dechlorination (**Table 2, entry 1**). The control experiments were done without catalyst and without current provided less dechlorination of PVC (**Table 2, entry 2 and 3**). With increasing temperature and time of the reaction, we experienced the dechlorination was enhanced (**Table 2, entry 4–9**) and best result we found at 60 °C with 15 h of CCE at 10 mA with complex **1**, got 91% of dechlorination (**Table 2, entry 8**). High temperature at 80 °C yielded 95% of dechlorination with 8 h of electrolysis (**Table 2, entry 9**).

Table 2. Reaction conditions of PVC dechlorination.

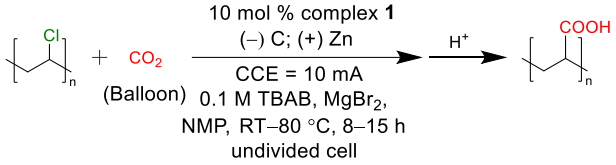

Entry	Conditions Variant	Dechlorination (%)
1	RT, 15 h	5
2	w/o complex **1**, 80 °C, 15 h	15
3	w/o current, 80 °C, 15 h	27
4	40 °C, 8 h	35
5	40 °C, 15 h	31
6	40 °C, 40 h	46
7	60 °C, 8 h	57
8	60 °C, 15 h	91
9	80 °C, 8 h	95

The incorporation of carboxylic acid and dechlorination of PVC was confirmed by attenuated total reflection Fourier transform infrared (FTIR) spectroscopy. The ATR spectra of PVC before and after the electrolysis was shown at **Figure 11**. The absence of C–Cl stretching frequency at 606 cm^{-1} was observed in the post electrolysis PVC and a new stretching

frequency was generated at 1697 cm^{-1} indicating the incorporation of acid unit (C=O stretching band) in the product. The percentage dechlorination of PVC was calculated using IC measurement of post electrolysis solution before acidification (**Figure S18**). This result provides the effectiveness of complex **1** is effective towards PVC C–Cl activation and functionalization.

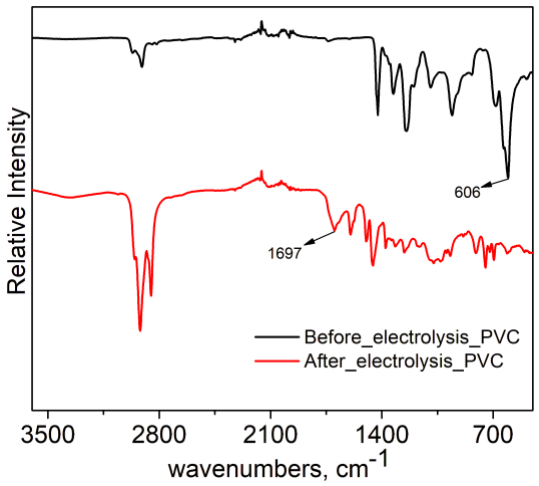

Figure 11. ATR spectra of before and after electrolysis of PVC.

3. Conclusions

The first electrochemical carboxylation of unactivated alkyl chlorides with CO_2 using Ni pincer complex (**1**) was developed. Herein, we demonstrate a simple and robust technique for synthesizing valuable carboxylic acids using undivided cells and also expands the applications towards PVC C–Cl activation and functionalization. Cross-coupling carboxylation over homocoupling of benzyl chlorides was achieved using a Ni-NNN (complex **1**) electrocatalyst to convert a variety of alkyl chlorides to acids at room temperature in good yields. Electronic structure calculations and electrochemical experiments were employed to elucidate the reaction mechanism. Starting with two subsequent ligand and metal-based reductions at –1.22 V and –1.59 V vs. Fc/Fc^{+}, the neutral Ni(II)-NNN pincer catalyst is converted to the active Ni(I)-catalyst. CO_2 binding mediated by the electron-rich ligand, followed by a third and fourth reduction at –1.90 V and -2.08 V, sets up the system for C-Cl bond activation. The last step has an activation energy of 19.3 kcal/mol. Reduced density gradient analysis revealed non-covalent interactions between the substrate and the imine ligand, which were hypothesized to stabilize the transition state for C–Cl bond cleavage. Based on ligand involvement in the proposed electrocarboxylation mechanism, future investigations will focus on preparing new redox-active ligand-based nickel complexes to transform secondary and tertiary alkyl chlorides into

carboxylic acids. The successful application of complex **1** on PVC upgrading demonstrates the vide applicability of the catalyst.

4. Acknowledgments

This work is supported by National Science Foundation under Grant No. CHE-2041436. Research reported in this publication was supported by the National Institute of General Medical Sciences of the National Institutes of Health under Award Number R15GM131290. The content is solely the responsibility of the authors and does not necessarily represent the official views of the National Institutes of Health. NMR experiments were performed on a Bruker AVANCE NEO 400MHz NMR spectrometer funded by NSF-MRI grant CBET-2051260. Funding for the D8 Venture diffractometer was through NSF-MRI grant CHE-1625737. Electronic structure calculations were carried out on Spiedie HPC at Binghamton University.

Supporting Information

Syntheses and characterization, procedures for the electrochemical studies, and DFT calculations. CCDC-2270473-2270474 contains the supplementary crystallography data for this paper. The data can be obtained free of charge from The Cambridge Crystallographic Data Centre via www.ccdc.cam.ac.uk/data_request/cif. The Supporting Information is available free of charge on the ACS Publications website.

AUTHOR INFORMATION

Corresponding Author

Jianbing "Jimmy" Jiang – Department of Chemistry, University of Cincinnati, P.O. Box 210172, Cincinnati, Ohio 45221, United States; https://orcid.org/0000-0002-7466-522X; Email: jianbing.jiang@uc.edu

Julien Panetier – Department of Chemistry, State University of New York at Binghamton, Binghamton, NY 13902 United States; https://orcid.org/0000-0003-4905-8396; Email: panetier@binghamton.edu

Authors

Prasenjit Sarkar – Department of Chemistry, University of Cincinnati, P.O. Box 210172, Cincinnati, Ohio 45221-0172, United States; https://orcid.org/0000-0003-4844-8421;

Sandeep Dash – Department of Chemistry, State University of New York at Binghamton, Binghamton, NY 13902 United States; https://orcid.org/0000-0003-1711-6141;

Jeanette A. Krause – Department of Chemistry, University of Cincinnati, Cincinnati, Ohio 45221, United States;

5. References

(1) Krische, M. J., *Metal Catalyzed Reductive C–C Bond Formation*. Springer: 2007.
(2) Chen, H.; Yue, H.; Zhu, C.; Rueping, M., Reactivity in Nickel-Catalyzed Multi-Component Sequential Reductive Cross-Coupling Reactions. *Angew Chem Int Ed* **2022**, *61*, e202204144.
(3) Jia, X. G.; Yao, Q. W.; Shu, X. Z., Enantioselective Reductive N-Cyclization-Alkylation Reaction of Alkene-Tethered Oxime Esters and Alkyl Iodides by Nickel Catalysis. *J Am Chem Soc* **2022**, *144*, 13461-13467.
(4) Liu, J.; Ye, Y.; Sessler, J. L.; Gong, H., Cross-Electrophile Couplings of Activated and Sterically Hindered Halides and Alcohol Derivatives. *Acc Chem Res* **2020**, *53*, 1833-1845.
(5) Lucas, E. L.; Jarvo, E. R., Stereospecific and Stereoconvergent Cross-Couplings between Alkyl Electrophiles. *Nat Rev Chem* **2017**, *1*.
(6) Wang, F.; Pan, S.; Zhu, S.; Chu, L., Selective Three-Component Reductive Alkylalkenylation of Unbiased Alkenes Via Carbonyl-Directed Nickel Catalysis. *ACS Catal* **2022**, *12*, 9779-9789.
(7) Parasram, M.; Shields, B. J.; Ahmad, O.; Knauber, T.; Doyle, A. G., Regioselective Cross-Electrophile Coupling of Epoxides and (Hetero)Aryl Iodides Via Ni/Ti/Photoredox Catalysis. *ACS Catal* **2020**, *10*, 5821-5827.
(8) Peng, L.; Li, Z.; Yin, G., Photochemical Nickel-Catalyzed Reductive Migratory Cross-Coupling of Alkyl Bromides with Aryl Bromides. *Org Lett* **2018**, *20*, 1880-1883.
(9) Smith, R. T.; Zhang, X.; Rincon, J. A.; Agejas, J.; Mateos, C.; Barberis, M.; Garcia-Cerrada, S.; de Frutos, O.; MacMillan, D. W. C., Metallaphotoredox-Catalyzed Cross-Electrophile Csp3-Csp3 Coupling of Aliphatic Bromides. *J Am Chem Soc* **2018**, *140*, 17433-17438.
(10) Xi, X.; Luo, Y.; Li, W.; Xu, M.; Zhao, H.; Chen, Y.; Zheng, S.; Qi, X.; Yuan, W., From Esters to Ketones Via a Photoredox-Assisted Reductive Acyl Cross-Coupling Strategy. *Angew Chem Int Ed* **2022**, *61*, e202114731.
(11) Xia, Q.; Dong, J.; Song, H.; Wang, Q., Visible-Light Photocatalysis of the Ketyl Radical Coupling Reaction. *Chemistry* **2019**, *25*, 2949-2961.
(12) Yu, W.; Chen, L.; Tao, J.; Wang, T.; Fu, J., Dual Nickel- and Photoredox-Catalyzed Reductive Cross-Coupling of Aryl Vinyl Halides and Unactivated Tertiary Alkyl Bromides. *Chem Commun* **2019**, *55*, 5918-5921.
(13) Zhang, P.; Le, C. C.; MacMillan, D. W., Silyl Radical Activation of Alkyl Halides in Metallaphotoredox Catalysis: A Unique Pathway for Cross-Electrophile Coupling. *J Am Chem Soc* **2016**, *138*, 8084-7.
(14) Jutand, A., Contribution of Electrochemistry to Organometallic Catalysis. *Chem Rev* **2008**, *108*, 2300-47.
(15) Qiu, Y.; Zhu, C.; Stangier, M.; Struwe, J.; Ackermann, L., Rhodaelectro-Catalyzed C–H and C–C Activation. *CCS Chem* **2021**, *3*, 1529-1552.
(16) Siu, J. C.; Fu, N.; Lin, S., Catalyzing Electrosynthesis: A Homogeneous Electrocatalytic Approach to Reaction Discovery. *Acc Chem Res* **2020**, *53*, 547-560.
(17) Yan, M.; Kawamata, Y.; Baran, P. S., Synthetic Organic Electrochemical Methods since 2000: On the Verge of a Renaissance. *Chem Rev* **2017**, *117*, 13230-13319.
(18) Woldu, A. R.; Huang, Z.; Zhao, P.; Hu, L.; Astruc, D., Electrochemical CO_2 Reduction (CO_2RR) to Multi-Carbon Products over Copper-Based Catalysts. *Coord Chem Rev* **2022**, *454*, 214340.
(19) Rafiq, M.; Hu, X.; Ye, Z.; Qayum, A.; Xia, H.; Hu, L.; Lu, F.; Chu, P. K., Recent Advances in Structural Engineering of 2d Hexagonal Boron Nitride Electrocatalysts. *Nano Energy* **2022**, *91*, 106661.
(20) Francke, R.; Little, R. D., Redox Catalysis in Organic Electrosynthesis: Basic Principles and Recent Developments. *Chem Soc Rev* **2014**, *43*, 2492-521.

(21) Wang, F.; Stahl, S. S., Electrochemical Oxidation of Organic Molecules at Lower Overpotential: Accessing Broader Functional Group Compatibility with Electron-Proton Transfer Mediators. *Acc Chem Res* **2020**, *53*, 561-574.
(22) Yakhvarov, D. G.; Khusnuriyalova, A. F.; Sinyashin, O. G., Electrochemical Synthesis and Properties of Organonickel σ-Complexes. *Organometallics* **2014**, *33*, 4574-4589.
(23) Davies, J.; Janssen-Muller, D.; Zimin, D. P.; Day, C. S.; Yanagi, T.; Elfert, J.; Martin, R., Ni-Catalyzed Carboxylation of Aziridines En Route to Beta-Amino Acids. *J Am Chem Soc* **2021**, *143*, 4949-4954.
(24) Jiao, K. J.; Liu, D.; Ma, H. X.; Qiu, H.; Fang, P.; Mei, T. S., Nickel-Catalyzed Electrochemical Reductive Relay Cross-Coupling of Alkyl Halides to Aryl Halides. *Angew Chem Int Ed* **2020**, *59*, 6520-6524.
(25) Fu, G. C., Transition-Metal Catalysis of Nucleophilic Substitution Reactions: A Radical Alternative to Sn1 and Sn2 Processes. *ACS Cent Sci* **2017**, *3*, 692-700.
(26) Gu, J.; Wang, X.; Xue, W.; Gong, H., Nickel-Catalyzed Reductive Coupling of Alkyl Halides with Other Electrophiles: Concept and Mechanistic Considerations. *Org Chem Front* **2015**, *2*, 1411-1421.
(27) Leon, T.; Correa, A.; Martin, R., Ni-Catalyzed Direct Carboxylation of Benzyl Halides with CO_2. *J Am Chem Soc* **2013**, *135*, 1221-4.
(28) Chen, B.-L.; Zhu, H.-W.; Xiao, Y.; Sun, Q.-L.; Wang, H.; Lu, J.-X., Asymmetric Electrocarboxylation of 1-Phenylethyl Chloride Catalyzed by Electrogenerated Chiral $[Co^{I}(Salen)]-$ Complex. *Electrochem commun* **2014**, *42*, 55-59.
(29) Borjesson, M.; Moragas, T.; Martin, R., Ni-Catalyzed Carboxylation of Unactivated Alkyl Chlorides with CO_2. *J Am Chem Soc* **2016**, *138*, 7504-7.
(30) Ang, N. W. J.; Oliveira, J. C. A.; Ackermann, L., Electroreductive Cobalt-Catalyzed Carboxylation: Cross-Electrophile Electrocoupling with Atmospheric CO_2. *Angew Chem Int Ed* **2020**, *59*, 12842-12847.
(31) Wang, L.; Li, T.; Perveen, S.; Zhang, S.; Wang, X.; Ouyang, Y.; Li, P., Nickel-Catalyzed Enantioconvergent Carboxylation Enabled by a Chiral 2,2'-Bipyridine Ligand. *Angew Chem Int Ed* **2022**, *61*, e202213943.
(32) Wu, L.-X.; Deng, F.-J.; Wu, L.; Wang, H.; Chen, T.-j.; Guan, Y.-B.; Lu, J.-X., Nickel-Catalyzed Electrocarboxylation of Allylic Halides with CO_2. *New J Chem* **2021**, *45*, 13137-13141.
(33) Corbin, N.; Yang, D. T.; Lazouski, N.; Steinberg, K.; Manthiram, K., Suppressing Carboxylate Nucleophilicity with Inorganic Salts Enables Selective Electrocarboxylation without Sacrificial Anodes. *Chem Sci* **2021**, *12*, 12365-12376.
(34) Sun, G. Q.; Zhang, W.; Liao, L. L.; Li, L.; Nie, Z. H.; Wu, J. G.; Zhang, Z.; Yu, D. G., Nickel-Catalyzed Electrochemical Carboxylation of Unactivated Aryl and Alkyl Halides with CO_2. *Nat Commun* **2021**, *12*, 7086.
(35) Patai, S., *The Chemistry of Acid Derivatives*. Wiley: New York: 1992.
(36) Maag, H., Prodrugs of Carboxylic Acids. **2007**, *V*, 703-729.
(37) Lamberth, C.; Dinges, J. In *Different Roles of Carboxylic Functions in Pharmaceuticals and Agrochemicals*, Wiley-VCH Verlag GmbH & Co. KGaA.: Weinheim: 2016; pp 1-11.
(38) Hazari, N.; Heimann, J. E., Carbon Dioxide Insertion into Group 9 and 10 Metal-Element Sigma Bonds. *Inorg Chem* **2017**, *56*, 13655-13678.
(39) Mei, T.-S.; Chen, Y.-G.; Xu, X.-T.; Zhang, K.; Li, Y.-Q.; Zhang, L.-P.; Fang, P., Transition-Metal-Catalyzed Carboxylation of Organic Halides and Their Surrogates with Carbon Dioxide. *Synthesis* **2017**, *50*, 35-48.
(40) Luan, Y.-X.; Ye, M., Transition Metal-Mediated or Catalyzed Hydrocarboxylation of Olefins with CO_2. *Tetrahedron Lett* **2018**, *59*, 853-861.
(41) Fujihara, T.; Tsuji, Y., Cobalt- and Rhodium-Catalyzed Carboxylation Using Carbon Dioxide as the C1 Source. *Beilstein J Org Chem* **2018**, *14*, 2435-2460.

(42) Tortajada, A.; Julia-Hernandez, F.; Borjesson, M.; Moragas, T.; Martin, R., Transition-Metal-Catalyzed Carboxylation Reactions with Carbon Dioxide. *Angew Chem Int Ed* **2018**, *57*, 15948-15982.
(43) Hong, J.; Li, M.; Zhang, J.; Sun, B.; Mo, F., C-H Bond Carboxylation with Carbon Dioxide. *ChemSusChem* **2019**, *12*, 6-39.
(44) Yang, Y.; Lee, J. W., Toward Ideal Carbon Dioxide Functionalization. *Chem Sci* **2019**, *10*, 3905-3926.
(45) Cao, Y.; He, X.; Wang, N.; Li, H.-R.; He, L.-N., Photochemical and Electrochemical Carbon Dioxide Utilization with Organic Compounds. *Chin J Chem* **2018**, *36*, 644-659.
(46) Paul, G. C.; Sarkar, P.; Mukherjee, C., Effect of H-Bond and Molecular Geometry Towards Innocent and Non-Innocent Behavior of 3,5-Di-Tert-Butyl-2-Aminophenol Units Attached to a Piperazine Backbone: Co(III) and Cu(II) Complexes. *Inorganica Chimica Acta* **2019**, *486*, 213-220.
(47) Anderson, J. S.; Iluc, V. M.; Hillhouse, G. L., Reactions of CO_2 and CS_2 with 1,2-Bis(Di-Tert-Butylphosphino)Ethane Complexes of Nickel(0) and Nickel(I). *Inorg Chem* **2010**, *49*, 10203-10207.